UDC 551.515.21:551.509.313

THE RESPONSE OF A TROPICAL CYCLONE MODEL TO VARIATIONS IN BOUNDARY LAYER PARAMETERS, INITIAL CONDITIONS, LATERAL BOUNDARY CONDITIONS, AND DOMAIN SIZE

STANLEY L. ROSENTHAL

National Hurricane Research Laboratory, Environmental Research Laboratories, NOAA, Miami, Fla.

ABSTRACT

Tropical cyclone model experiments are summarized in which the drag coefficient and the analogous exchange coefficients for sensible and latent heat are varied. During the early portions of the immature stage, the response of the model storm follows linear theory and growth is more rapid with larger drag coefficients. However, the ultimate intensity reached by model storms varies inversely with the drag coefficient. The experiments indicate that air-sea exchanges of latent heat are crucial for the development and maintenance of the model storm. The air-sea exchange of sensible heat appears to be far less important.

Experiments conducted with open lateral boundary conditions revealed that the structure and intensity of the mature stage of the model cyclone is relatively insensitive to the initial perturbation and to the size of the computational domain. The time required to reach the mature stage is, however, quite sensitive to these influences.

Comparisons between experiments with open and mechanically closed lateral boundaries show the lateral boundary conditions to be extremely important. For computational domains of 2000 km or less, model cyclones with closed lateral boundaries are less intense than their counterparts with open lateral boundaries. However, the intensity of the closed systems increases markedly with domain size and the experiments suggest that differences due to boundary conditions might be minimized if the domain size exceeded 2000 km.

1. INTRODUCTION

This paper summarizes a new series of experiments conducted with the circularly symmetric tropical cyclone model described by Rosenthal (1970*b*). Recent studies with a three-dimensional model (Anthes et al. 1971*a*, 1971*b*) indicate that many symmetric results can be extrapolated to the asymmetric case and, therefore, justify continued experimentation with symmetric models.

The new experiments are based on a version of the symmetric model which differs from that described by Rosenthal (1970*b*) only in one important aspect. Whereas air-sea exchanges of sensible and latent heat were previously simulated by some rather pragmatic constraints on the Ekman layer humidities and temperatures, these energy fluxes are now computed explicitly by the bulk aerodynamic method. Details are given in section 2.

Comparisons of the physical and numerical characteristics of this model and those of Ooyama (1969) and Yamasaki (1968) were presented earlier (Rosenthal 1970*b*) and need not be repeated here. More recently, a new symmetric model (Sundqvist 1970) has appeared in the literature. There are a number of differences between Sundqvist's model and ours; the most prominent of which is his use of the gradient wind assumption. In our system, the primitive equations govern the horizontal motion. Sundqvist works in the p-system in contrast to our z-system, but he has better vertical resolution (10 levels spaced at 100-mb intervals in contrast to our seven irregularly spaced levels). Radial resolution is 25 km in Sundqvist's model, while most of our calculations are performed with a radial increment of 10 km.

Section 2 of this paper gives a verbal description of the model and also presents the formulations of the air-sea exchanges of sensible and latent heat that have now been adopted. Section 3 describes a basic (control) experiment that serves as a comparison for the later experiments.

Section 4 is concerned with the interesting dual role played by surface drag friction in hurricane dynamics; frictional convergence of water vapor in the Ekman layer drives the organized cumulus convection but, on the other hand, drag friction at the air-sea interface is the prime dissipater of kinetic energy for mature tropical cyclones.

The still controversial problem (Dergarabedian and Fendell 1970) of the significance of air-sea exchanges of sensible and latent heat is the topic of section 5. In general, the experiments discussed in sections 4 and 5 qualitatively confirm conclusions reached by Ooyama (1969). In view of substantial differences in the physical and numerical details of the two models, their qualitative agreement is an important matter which lends credence to both models.

Section 6 is concerned with some of the more arbitrary aspects of the model such as lateral boundary conditions, initial conditions, and radial extent of the computational domain. Finally, section 7 reviews the main conclusions of the paper.

2. REVIEW OF THE MODEL

A brief description of the main features of the model is given below. The reader concerned with mathematical details should refer to Rosenthal (1970*b*). The vertical structure of the atmosphere is represented by seven levels and geometric height is the vertical coordinate. The levels correspond to pressures of 1015, 900, 700, 500, 300, 200, and 100 mb in the mean tropical atmosphere. All variables are defined at all levels. The primitive equations govern the horizontal motion. The hydrostatic assumption is employed.

The continuity equation is simplified as follows. The local rate of change of density is neglected and a climatological density (a function of height alone) is used to evaluate the vertical and horizontal mass flux terms. We then eliminate the external gravity wave by demanding

that the vertical integral of the horizontal mass divergence vanish.

In the control experiment, the radial limit of the computational domain is 440 km. The system is open at the lateral boundary. The lateral boundary conditions require the relative vorticity and horizontal divergence to vanish. In addition, the radial derivatives of potential temperature and specific humidity are also required to vanish.

Through a generalization of the procedure suggested by Kuo (1965), the model simulates convective precipitation (and the macroscale heating due to this latent heat release) as well as the enrichment of the macroscale humidity due to the presence of the cumuli. Convection may originate in any layer, provided that the layer has a water vapor supply from horizontal convergence and that conditional instability exists for parcels lifted from the layer. Nonconvective precipitation is also simulated. Details are given by Rosenthal (1970*b*).

Time derivatives are estimated by forward differences except in the case of specific humidity, where a Matsuno (1966)-type integration is employed. Advective derivatives are calculated by the upstream method except for the case of humidity, where a conservation form of the equations is used. All nonadvective space derivatives are calculated as centered differences.

Grid points in the radial direction are staggered. Horizontal velocity is defined at the radii

$$r_j=(j-1)\Delta r, \qquad j=1, 2 \ldots . \tag{1}$$

Temperature, pressure, vertical motion, and humidity are carried at the radii

$$r_j=(j-\tfrac{1}{2})\Delta r, \qquad j=1, 2 \ldots . \tag{2}$$

The constant drag coefficient (C_D) of 3×10^{-3} used in previous experiments (Rosenthal 1969, 1970*a*, 1970*b*) has been replaced with Deacon's empirical relationship (Roll 1965, p. 160). The latter may be written

$$C_D=1.1\times10^{-3}+4.0\times10^{-5}|V_{10}|. \tag{3}$$

The symbol $|V_{10}|$ denotes the wind speed 10 m above the sea surface. In the model, the sea-level wind is used to evaluate C_D.

The sensible and latent heat fluxes at sea level are calculated, respectively, from

$$F_s=[\bar{\rho}C_pC_S|V_{10}|(T_{sea}-T)]_{z=0} \tag{4}$$

and

$$F_l=[\bar{\rho}_LC_L|V_{10}|(q_{sea}-q)]_{z=0}. \tag{5}$$

Here, C_S and C_L are exchange coefficients for sensible and latent heat analogous to C_D, T_{sea} is the sea surface temperature, q_{sea} is the saturation specific humidity at the temperature and pressure of the sea. The remainder of the symbols are standard. Equation (4) is used only when $(T_{sea}-T)_{z=0}>0$. In other circumstances the flux is zero. When $(q_{sea}-q)_{z=0}<0$, the latent heat flux is zero.

In the basic experiment, $C_S=C_L=C_D$. The flux convergences that appear in the thermodynamic and water vapor continuity equations are evaluated through the assumption that the fluxes have a linear variation over height and are zero at and above the height of the 900-mb level. This is based on the assumption that at 900 mb and above, fluxes produced by small-scale turbulence are insignificant in comparison to those produced by cumulus-scale motions.

TABLE 1.—*Standard values of thermodynamic variables*

Level	Height	$\bar{\theta}$	$\bar{T}$	$\bar{p}$
	(m)	(°K)	(°K)	(mb)
1	0	300	301.3	1015.0
2	1,054	303	294.1	900.4
3	3,187	313	282.6	699.4
4	5,898	325	266.5	499.2
5	9,697	340	240.8	299.2
6	12,423	347	218.9	199.5
7	16,621	391	203.1	101.1

The sea temperature is an external parameter and, for experiments discussed here, is taken 2°K greater than the initial sea-level air temperature (the latter is initially horizontally uniform for all experiments). Since the sea-level air temperature varies with time according to the thermodynamic equation, the air-sea temperature difference varies both with radius and time as the model hurricane evolves. In our basic experiment (section 3), the sea-level air temperature approaches the sea temperature before rapid development begins. Subsequent experiments, as well as a recent linear analysis by Rodenhuis (1971), have indicated that an important aspect of the boundary layer is its static stability. The model yields a somewhat more rapid development (in comparison to the basic experiment, section 3) when the initial sea-level air temperature is taken 2°K warmer than in the basic experiment but with the same sea temperature.

3. THE BASIC EXPERIMENT (EXP. S35)

The initial conditions for this experiment are those used for our previous (Rosenthal 1970*b*) calculations. They are established as follows. A field of standard potential temperatures [a function of height alone and almost identical to those of the Hebert and Jordan (1959) mean hurricane season sounding] is specified. With a lower boundary condition of 1015 mb, hydrostatic standard pressures and temperatures (table 1) are computed for the levels above the surface.

The initial temperature field is then specified by

$$T_{i,j}=\bar{T}_i+T_*\left(\cos\frac{\pi}{\hat{r}}r_j+1\right)\sin\frac{\pi}{z_7}z_i \tag{6}$$

where i and j are, respectively, height and radial indices, $\bar{T}_i$ is the standard temperature, $T_*=0.16$°K, $\hat{r}=440$ km, and z_7 is the height of level 7. These are given in table 1. The initial pressure at level 7 is then taken to be the standard value and the hydrostatic equation is integrated downward to obtain the remainder of the initial pressure field. Finally, the gradient wind equation is solved for the initial tangential wind while the initial radial and

TABLE 2.—*Initial values of relative humidity at the information levels*

Level	Height	Relative humidity
	(m)	(%)
1	0	90
2	1,054	90
3	3,187	54
4	5,898	44
5	9,697	30
6	12,423	30
7	16,621	30

vertical motions are taken to be zero. A base state relative humidity is specified as a function of height (table 2). By use of the data given in table 1, a base state specific humidity is calculated. The initial specific humidity is then assumed horizontally homogeneous and equal to this base state value.

The initial surface wind reaches a maximum of 7 m/s at a radius of 250 km. The central pressure of the vortex is 1013 mb. Since the initial conditions are clearly arbitrary, the early portions of the time integration are not particularly significant. This matter will be reconsidered later.

Radial resolution for the basic experiment is 10 km and the time step is 2 min. A lateral mixing coefficient of $2.5\times10^{3}\text{m}^2\cdot\text{s}^{-1}$ is used for momentum, heat, and water vapor.

Figure 1 summarizes the control storm's evolution at sea level.[1] The "organizational" period is about twice as long as that found in our previously published results (Rosenthal 1970*b*). This is primarily a result of replacing the constant drag coefficient (3×10^{-3}) with the variable C_D given by eq (3). Linear analysis (Ooyama 1969, Rosenthal and Koss 1968) shows growth rates for models of this general type to be directly proportional to the drag coefficient. From eq (3), the largest C_D at the initial instant is about 1.38×10^{-3} and this is less than half the constant 3×10^{-3} used in the previous calculations. Equation (3) does not yield a C_D of 3×10^{-3} until a wind of 47.5 m/s is reached.

The time needed for the model cyclone to become organized is also highly sensitive to the arbitrary initial conditions. Rosenthal (1970*b*) showed that enrichment of the initial humidity field could shorten the organizational period by several days. Ooyama (1969) showed that variations of the scale of the initial perturbation strongly affected the length of this period while Anthes et al. (1971*b*) showed a relationship between the intensity of the initial perturbation and the length of the organizational period. The latter is revealed by figure 2 where we show the result of an experiment (Q2) in which T_*[eq (6)] was three times the value used for the control experiment. This provided a maximum initial wind approximately twice that of the control. The organizational period for Q2 is only 24 hr and peak intensity is reached at 120 hr.

[1] Pressure is not defined at zero radius because of the grid staggering [eq (1) and (2)]. Central pressure values presented in this paper are pressure values at $z=0$, $r=\Delta r/2$.

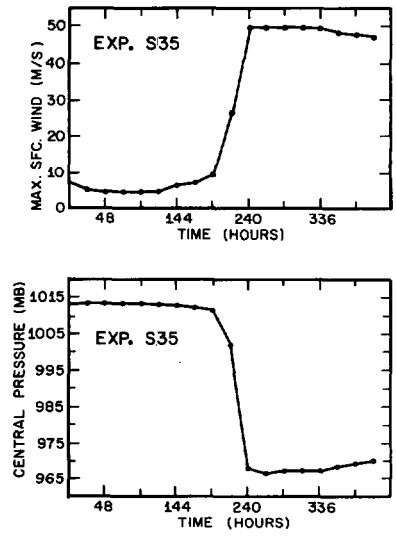

FIGURE 1.—Results from experiment S35. (Top) maximum surface wind as a function of time and (bottom) central pressure as a function of time.

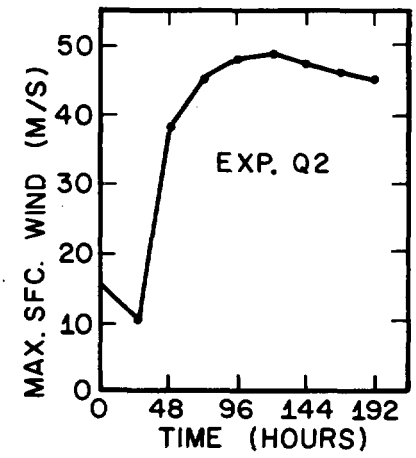

FIGURE 2.—Maximum surface wind as a function of time for experiment Q2. The initial maximum surface wind for this experiment is twice as strong as for the control.

Despite differences in the histories, the peak intensities for S35 and Q2 differ only by 1.5 m/s.

The material presented in the last few paragraphs indicates that the length of the organizational period, as given by model calculations, is only of significance when experiments are compared against each other. Ramage's (1970) comments concerning the unrealistic length of the organizational period of some of Ooyama's (1969) experiments would, therefore, appear to be irrelevant since Ooyama's calculations are based on hypothetical initial data. Ramage's point, of course, will become highly pertinent when models reach a level of sophistication that justifies their application to real data.

Figures 3, 4, 5, 6, and 7 illustrate structural features of the basic experiment (at 312 hr) that are representative of the period between 240 and 336 hr. The wind field (fig. 3), while similar to those obtained previously, is somewhat smoother and the thermal structure (fig. 4) is substantially improved (cf. fig. 7, Rosenthal 1970*b*). The weak warm center at low elevations and large radii is produced by sub-

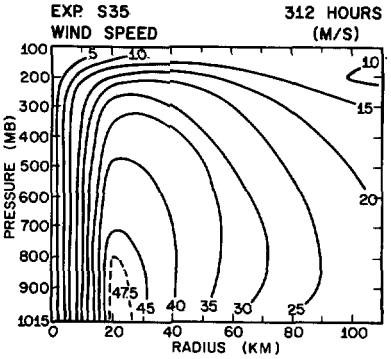

FIGURE 3.—Cross section of wind speed at hour 312 of experiment S35. Isotachs are labeled in m/s.

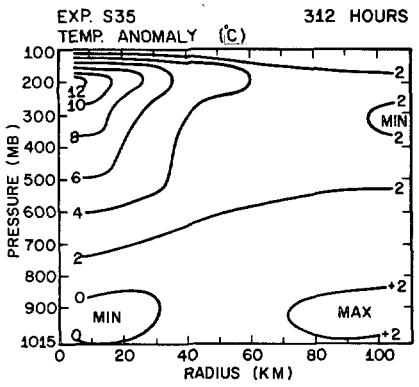

FIGURE 4.—Cross section of temperature anomalies at hour 312 of experiment S35. Isotherms are labeled in °C.

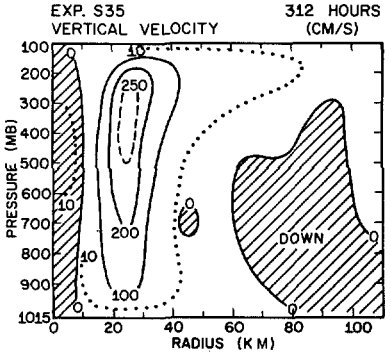

FIGURE 5.—Cross section of vertical velocity at hour 312 of experiment S35. Isotachs are labeled in cm/s. Hatched areas indicate negative values (subsidence).

sidence (fig. 5) while the low-level cool pocket near the storm center is a result of a slight excess of adiabatic cooling over the sum of the convective heating and the air-sea exchange of sensible heat. We note that empirical evidence in support of low-level cold pockets near the storm center exists (Hawkins and Rubsam 1968, Colón et al. 1961). The vertical motions (fig. 5) show a more distinct region of subsidence ("eye") at the storm center than found in our previous experiments.

The relative humidity (fig. 6) shows saturation in the region of major upward motion. This region is an analog to the eye wall. An upper tropospheric tongue of saturation extends outward to large radii and appears to be analogous to the cirrus canopy. The humidity pattern is highly

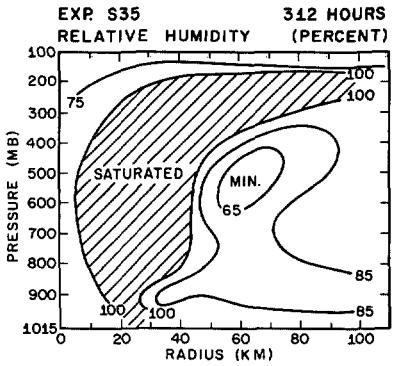

FIGURE 6.—Cross section of relative humidity (percent) at hour 312 of experiment S35. Saturated areas are hatched.

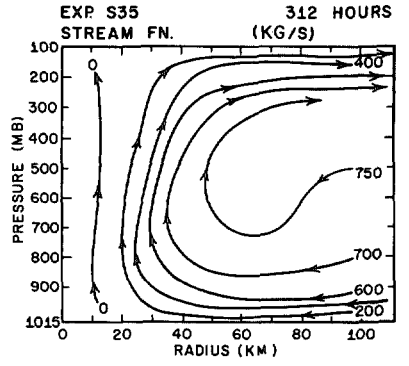

FIGURE 7.—Cross section of the mass transport Stokes' stream function at hour 312 of experiment S35. Streamlines are labeled in kg/s. No streamlines are drawn inside the 10-km radius.

correlated to the meridional circulation as revealed by the Stokes' stream function for mass transport (fig. 7).

The midtropospheric humidity minimum near 60-km radius is very nearly coincident with the circulation center revealed by figure 7. Relative humidity values in this region are only 20 percent or so greater than the initial values. The dry tongue extending to large radii at low elevations is associated with the subsidence already noted.

Detailed histories of various integral properties are not presented since these are similar to those previously published (Rosenthal 1970*b*). Tables 3 and 4 do, however, make some comparisons between the mature stage of the model and that of hurricane Daisy (1958). The data for hurricane Daisy are taken from Riehl and Malkus (1961). In view of the observational uncertainties in the empirical estimates and the natural storm-to-storm variability [cf. estimates by Riehl and Malkus (1961) with Hawkins and Rubsam (1968) and Miller (1962)], the agreement between the model values and those for hurricane Daisy is as good as can be expected.

4. DUAL ROLE OF THE DRAG COEFFICIENT

Linear analysis shows growth rates to be directly proportional to the drag coefficient, as already noted, and to the boundary layer humidity (Ooyama 1969, Rosenthal and Koss 1968). From the point of view of water vapor supply, this result is entirely logical since the primary

TABLE 3.—*Sensible heat flux and evaporation rates for 1958 hurricane Daisy and experiment S35 at 312 hr. Rainfall rates for experiment S35 are also shown.*

	Average model values for radial interval 0–100 km at 312 hr	Average values for hurricane Daisy for radial interval 0–80 n.mi. on Aug. 27, 1958
Sensible heat flux (cal · cm^{-2} · s^{-1})	1.5×10^{-3}	2.9×10^{-3}
Evaporation (cm/day)	1.8	2.3
Rainfall (cm/day)	22	

TABLE 4.—*Kinetic energy generation and dissipation by surface drag friction for 1958 hurricane Daisy and experiment S35 at 312 hr*

	Integrated values from model for radial interval 0–100 km at 312 hr	Integrated values for hurricane Daisy for radial interval 0–60 n.mi. on Aug. 27, 1958
Kinetic energy production (10^{14} kJ/day)	5.8	4.6
Kinetic energy dissipation by surface friction (10^{14} kJ/day)	2.9	2.1

TABLE 5.—*Experiments in which the drag coefficient is varied during the immature stage of the model cyclone. The initial data for these experiments are from hour 168 of experiment S35.*

Experiment	C_D	$C_S=C_L=C_E$	C_D/C_E
S35	eq (3)	eq (3)	1
Q3	2Xeq (3)	do.	2
Q5	5Xeq (3)	do.	5
Q17	0.75Xeq (3)	do.	3/4
Q20	0.20Xeq (3)	do.	1/5

source of water vapor for the organized cumulus convection is frictional convergence in the Ekman boundary layer. On the other hand, increased surface drag also leads to an increased dissipation of kinetic energy.

Apparently, in the earlier stages of development where linear theory is valid, increased water vapor convergence dominates increased dissipation (provided that the static stability is not too large) and growth rates increase with increasing drag coefficients.

However, as growth rates are increased through increases of the drag coefficient, the nonlinear effects should become significant earlier in the life cycle and linear theory should fail at an earlier point in the evolution of the cyclone. As a result, linear theory in itself is not sufficient for determining whether the ultimate intensity of the model cyclone will vary directly or indirectly with the drag coefficient. For this answer, we must resort to numerical experimentation. Ooyama's (1969) experiments indicate that the ultimate intensity decreases as the drag coefficient increases and the results of our experiments provide a similar conclusion.

In the first group of these experiments, C_D was varied during the linear phase of the system. The initial data for these experiments are taken from hour 168 of the control. The calculations were continued from this point with the modifications in drag coefficient shown by table 5 and do not differ from S35 in any other way. In particular, the exchange coefficients for latent and sensible heat are evaluated as they were in the control [eq (3)].

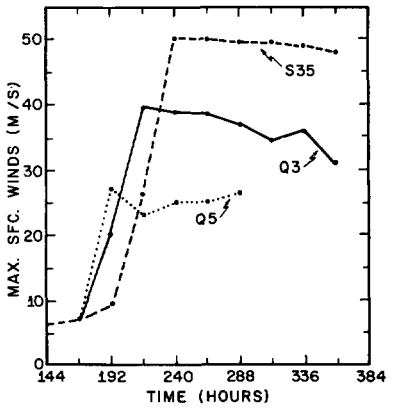

FIGURE 8.—Comparison of the maximum surface wind for experiment S35 with those for experiment Q3 [C_D twice the value given by eq (3)] and Q5 [C_D five times the value given by eq (3)]. See table 5 for details. Initial data for Q3 and Q5 are taken from hour 168 of S35.

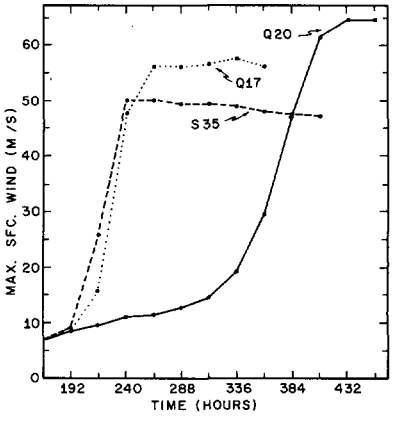

FIGURE 9.—Comparison of maximum surface wind for experiment S35 with those for experiments Q17 [$C_D=0.75$ of the value given by eq (3)] and Q20 [$C_D=0.20$ of value given by eq (3)]. See table 5 for details. Initial data for Q17 and Q20 are taken from hour 168 of S35.

Figure 8 shows the result of increasing[2] C_D (exp. Q3 and Q5) and, clearly, the early portions of these calculations behave as predicted by linear theory. On the other hand, as suggested by the arguments earlier in this section, linear theory becomes invalid sooner with increasing C_D and peak intensities are inversely related to the drag coefficient. Figure 9 verifies that decreased drag coefficients (exp. Q17 and Q20) lead to smaller growth rates but greater peak intensities. However, we should expect no growth at all when C_D is decreased to zero.

A similar series of experiments for the mature stage of the storm is summarized by table 6. Here, the initial data are from hour 288 of the basic experiment. Increasing the drag coefficient (fig. 10) results in a weakening of the storm which appears to vary directly with the amount by which C_D is raised (exp. Q4 and Q6). It is noted that the latent heat release (rainfall) and the kinetic energy generation are larger in Q4 and Q6 than in the control.

[2] For ease of expression, we will use terms such as "increase C_D," "double C_D," etc. Since C_D is wind dependent [eq (3)], these terms may not be quite accurate. What we, in fact, mean is that the constants in eq (3) are increased, doubled, etc.

TABLE 6.—*Experiments in which the drag coefficient is varied during the mature stage of the model cyclone. The initial data are from hour 288 of experiment S35.*

Experiment	C_D	$C_S=C_L=C_E$	C_D/C_E
S35	eq (3)	eq (3)	1
Q4	2Xeq (3)	do.	2
Q6	5Xeq (3)	do.	5
Q15	0	do.	0
Q19	0.75Xeq (3)	do.	3/4

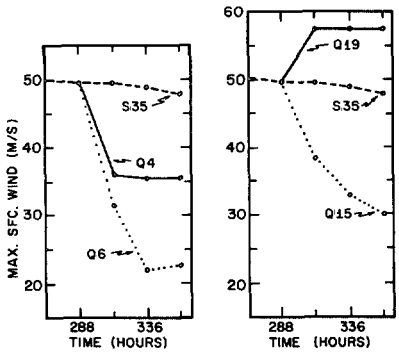

FIGURE 10.—Comparison of maximum surface wind for experiment S35 with those for experiment Q4 [C_D twice the value given by eq (3)], Q6 [C_D five times the value given by eq (3)], Q15 ($C_D=0$), and Q19 [$C_D=0.75$ of value given by eq (3)]. See table 6 for details. Initial data taken from hour 288 of S35.

When the drag coefficient is reduced by 25 percent (exp. Q19, fig. 10), the maximum surface winds rise by about 7 m/s. However, experiment Q15 ($C_D=0$) indicates that a continued decrease in C_D will not result in ever stronger peak winds.

The response of the mature model storm to changes of C_D is then fairly complex. Increased drag coefficients lead to greater rainfall and latent heat release but to weaker peak winds due to increased dissipation. If the drag coefficient is decreased, the maximum winds increase unless C_D is made so small that the water vapor convergence at low levels becomes the dominant factor. In this case, reductions in drag coefficient result in reductions in the maximum winds.

5. AIR-SEA EXCHANGE OF SENSIBLE AND LATENT HEAT

Air-sea exchanges of sensible and latent heat have long been considered important ingredients in the development and maintenance of tropical storms. Palmén (1948) showed, on a climatological basis, that tropical storms form primarily over warm ocean waters ($T_{sea}>26$°C). Malkus and Riehl (1960) showed that the deep central pressures associated with hurricanes could not be explained hydrostatically unless the equivalent potential temperature, θ_e, in the boundary layer was 10° to 15°K greater than that of the mean tropical atmosphere. Byers (1944) pointed out that the observed near-isothermal conditions for inward spiraling air in the hurricane boundary layer required a source of sensible heat to compensate for the cooling due to adiabatic expansion. Ooyama (1969) argued that if the θ_e of the boundary layer remained constant, the conditional instability near the storm center would soon be decreased as the storm's warm core developed and that the vertical mean temperatures of atmospheric columns would be unlikely to increase further once the lapse rate became moist neutral.

Despite these arguments and observations, the evaporation rates for hurricanes are very small compared to the lateral inflows of water vapor and, furthermore, the air-sea exchange of sensible heat is only a few percent of the latent heat release (Riehl and Malkus 1961, Malkus and Riehl 1960). As a result, controversy over the importance of these boundary layer processes continues (Dergarabedian and Fendell 1970).

Ooyama (1969) found drastic reductions in the strength of his model storm when the air-sea exchanges of sensible and latent heat were suppressed. He pointed out that at sufficiently large radii, the boundary layer is divergent (the so-called Ekman layer "sucking"). Examples of this feature from our model are illustrated by figures 5 and 7. This subsidence tends to decrease the boundary layer θ_e since $\partial\theta_e/\partial z<0$ in the lower troposphere. Ooyama argued that unless the energy supply from the ocean can again raise the θ_e of the boundary layer air to sufficiently large values before the inflowing air reaches the inner region, the convective activity will diminish in those regions and, hence, the storm will begin to weaken.

Ooyama's line of reasoning can be extended to show that evaporation is far more important than sensible heat flux. The air sucked into the boundary layer has a higher potential temperature than the original boundary layer air. The subsiding air has a smaller θ_e only because it is relatively dry.

Experiments appropriate to the immature stage of the model storm are summarized by table 7. Results are given by figure 11. During the first 48 hr, the only experiments in this group that depart significantly from the control are those for which C_D was altered (Q10 and Q18). This is consistent with the linear theory described in the previous section and again verifies that frictional convergence of water vapor is the most crucial factor during the early stages of development. The small growth shown by experiment Q10 ($C_D=0$) is a result of the meridional circulation already established in experiment S35 and which, therefore, is present in the initial data for Q10. Experiment Q18 is nearly identical to Q3 (table 5 and fig. 8) in which only C_D was doubled. In experiment Q11 where C_S and C_L are doubled while C_D is left as in the control, significant departures from the control are noted only after the mature stage is reached.

Experiments Q8 ($C_S=0$) and Q9 ($C_L=0$) support the extension of Ooyama's argument offered earlier. When the sensible heat flux is suppressed, the model storm develops a peak intensity of 45 m/s in comparison to 50 m/s for the control. When evaporation is suppressed, the peak intensity is only 22 m/s.

Experiments for the mature stage are listed in table 8 and results are summarized by figure 12. Suppression of

TABLE 7.—*Experiments that examine the relative importance of air-sea exchanges of sensible heat, latent heat, and momentum during the immature stage of the model cyclone. The initial data are from hour 168 of experiment S35.*

Experiment	C_D	C_S	C_L
S35	eq (3)	eq (3)	eq (3)
Q8	do.	0	do.
Q9	do.	eq (3)	0
Q10	0	do.	eq (3)
Q11	eq (3)	2Xeq (3)	2Xeq (3)
Q18	2Xeq (3)	do.	do.

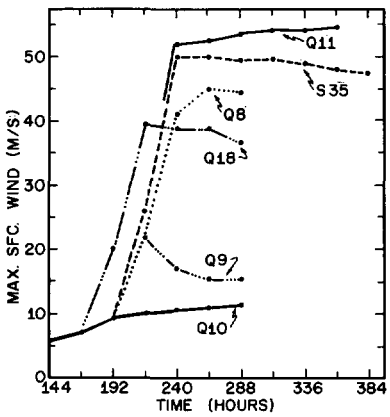

FIGURE 11.—Comparison of maximum surface winds for experiments that study the relative importance of air-sea exchanges of sensible heat, latent heat, and momentum during the immature stage of the model cyclone. Initial data are taken from hour 168 of experiment S35. The experiments compared with the control are Q8 ($C_S=0$), Q9 ($C_L=0$), Q10 ($C_D=0$), Q11 ($C_S=C_L=2C_D$), and Q18 ($C_S=C_L=0.5C_D$). See table 7 for details.

the evaporation (exp. Q14) again leads to a more dramatic response than does cutting off the sensible heat supply (Q13). In contrast to the immature stage, a greater departure from the control occurs in Q14 ($C_L=0$) than in Q15 ($C_D=0$). This is due to the presence of a well-marked Ekman layer convergence in the initial data. The latter is able to maintain itself for some time after C_D is set to zero. Indeed, as noted in section 4, *small* reductions in the drag coefficient during the mature stage lead to an *intensification* of the system (exp. Q19, fig. 10, table 6).

Experiment Q16 ($C_S=C_L=2C_D$) shows the type of response to be expected of a mature hurricane moving over warmer waters.

Despite the qualitative similarity of the wind maxima curves for Q14 and Q15 (fig. 12), the structural changes of the model storms are very different. In experiment Q14 where evaporation is suppressed, winds decrease everywhere and the area covered by strong winds decreases in size. This is illustrated by figure 13 where the outer radial limit of gale-force winds (approx. 17 m/s) is plotted as a function of time. In contrast, when the surface drag is suppressed (Q15), the area covered by strong winds expands (fig. 13) as the peak wind decreases. This, of course, is due to the fact that air spiraling inward does not lose momentum to the sea and, hence, reaches a particular

TABLE 8.—*Experiments that examine the relative importance of air-sea exchanges of sensible heat, latent heat, and momentum during the mature stage of the model cyclone. The initial data are from hour 288 of experiment S35.*

Experiment	C_D	C_S	C_L
S35	eq (3)	eq (3)	eq (3)
Q13	do.	0	do.
Q14	do.	eq (3)	0
Q15	0	do.	eq (3)
Q16	eq (3)	2Xeq (3)	2Xeq (3)

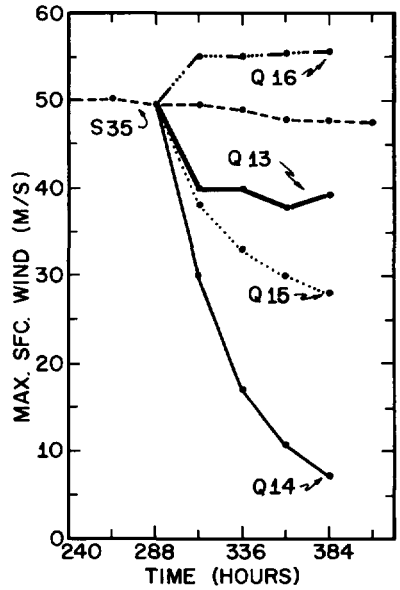

FIGURE 12.—Comparison of maximum surface winds for experiments that study the relative importance of air-sea exchanges of sensible heat, latent heat, and momentum during the mature stage of the model cyclone. Initial data are taken from hour 288 of experiment S35. The experiments compared with the control are Q13 ($C_S=0$), Q14 ($C_L=0$), Q15 ($C_D=0$), and Q16 ($C_S=C_L=2C_D$). See table 8 for details.

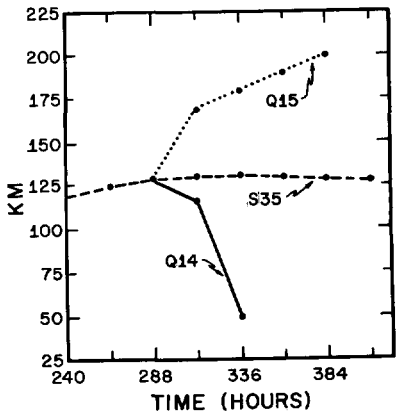

FIGURE 13.—Histories of the outer radial limit of gale-force winds for experiment Q15 ($C_D=0$), Q14 ($C_L=0$), and S35 (control). See table 8 for details.

radius with tangential winds greater than those found in the control.

The last two experiments to be discussed in this section are intended to simulate the passage of a mature hurricane

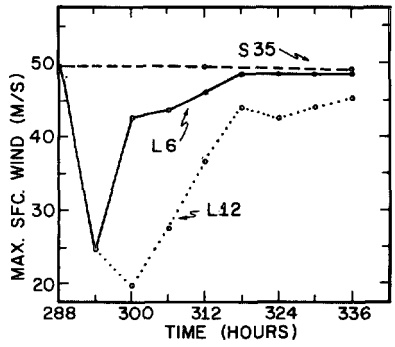

FIGURE 14.—Maximum surface winds as a function of time for experiment L6 and L12. These experiments are intended to simulate a hurricane that makes landfall at hour 288. In L6, the storm is over land for 6 hr and returns to water at hour 294. In L12, the storm is over land for 12 hr and returns to water at hour 300.

over an island. The initial data are again from hour 288 of experiment S35. In experiment L6, we set $C_S=C_L=0$ and $C_D=10^{-2}$ for 6 hr and then restore the original evaluations for these quantities. Experiment L12 differs only in that the modified exchange coefficients are retained for 12 hr before the original formulations are restored. Experiment L6 is then intended to represent a hurricane which spends 6 hr over land before returning to the sea while L12 is intended to simulate a 12-hr stay over land with a subsequent return to water.

The results, summarized by figure 14, show rapid filling upon "land fall." Comparisons of L6 and L12 show the filling to be most rapid during the earlier portion of the storm's land fall. Reintensification is rapid when the storm returns to "water." In experiment L6, the storm recovers its original intensity and structure (not shown) within 24 hr of its return to water. In experiment L12, the recovery is somewhat slower but the intensity appears to be approaching that of the control when the calculation is terminated. The storm structure for L12 at hour 336 (not shown) is very much like that of the control.

6. SOME ARBITRARY ASPECTS OF THE MODEL

Earlier, we pointed out that the length of the organizational period was extremely sensitive to variations in the initial conditions. This point will receive further attention below. We will also discuss two other arbitrary aspects of the model, the radial extent of the computational domain and the lateral boundary conditions.

In the first group of experiments (table 9), the computational domain is enlarged (exp. C16) and the scale of the initial perturbation is decreased (exp. Q1). To initialize C16, eq (6) is used for the inner 440 km. Beyond this radius, the initial temperatures are the standard values (table 1). As a result, the initial conditions for the inner 440 km are identical to the control. Beyond 440 km, the initial conditions are those of a stagnant mean tropical atmosphere. For experiment Q1, eq (6) with $\hat{r}=220$ km is used for the inner 220 km and $T_{i,j}=\overline{T}_i$ is used for the outer 220 km. This leads to a stagnant mean tropical atmosphere at radii greater than 220 km.

TABLE 9.—*Experiments in which the size of the computational domain (C16) and the horizontal scale of the initial perturbation (Q1) are varied*

Experiment	Domain size	Perturbation size	Initial maximum wind
	(km)	(km)	(m/s)
S35	440	440	7
C16	1000	440	7
Q1	440	220	6

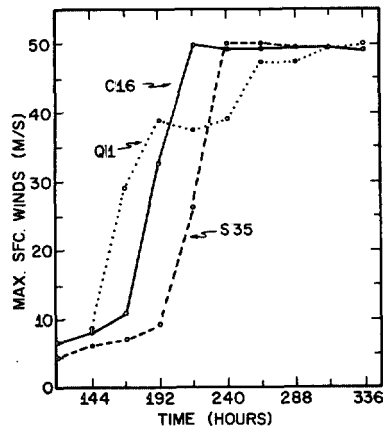

FIGURE 15.—Maximum surface winds for experiment C16 (computational domain 1000 km in comparison to 440 km for S35) and experiment Q1 (initial perturbation half as large in horizontal extent as that for S35). See table 9 for details.

The maximum surface winds for these experiments (fig. 15) approach those of the control. The evolution of experiment C16 indicates that moving the lateral boundary outward relative to the initial perturbation allows the storm to reach the mature stage more rapidly. Experiment Q1 introduces two conflicting effects. By reducing the scale of the initial perturbation, the active perturbation is removed from the lateral boundary in a fashion somewhat analogous to C16. However, this reduction in scale also increases the importance of the lateral mixing terms (Ooyama 1969). The calculations show Q1 to have a period in which growth is more rapid than the control, followed by a longer period in which growth is slow and uncertain. This model storm does not reach a mature steady state until well after the control does. Qualitatively similar results were obtained by Ooyama (1969).

Despite the evolutionary differences, table 10 shows the mature stages of the three model cyclones to be remarkably similar. We tentatively conclude that the structure and intensity of the mature stage is relatively insensitive to the size of the computational domain and the scale of the initial perturbation[3] with the boundary conditions used here. The time required to reach the mature stage, however, is highly sensitive to these parameters. In section 3, similar results were obtained when the intensity of the initial perturbation was varied (exp. Q2, fig. 2).

[3] It must, however, be kept in mind that, if the initial perturbation is made sufficiently small in scale, the lateral mixing terms will become dominant and, according to linear theory, the system will decay rather than grow.

TABLE 10.—*Summary of surface structure at hour 336 of experiments S35, Q1, and C16*

Experiment	Radius of maximum wind	Outer limit of hurricane-force winds	Outer limit of gale-force winds
	(km)	(km)	(km)
S35	20	55	130
Q1	20	55	125
C16	20	55	130

TABLE 11.—*Experiments (20-km radial resolution) which compar the effects of domain size and lateral boundary conditions*

Experiment	Domain size	Lateral boundary condition	Initial perturbation
	(km)		
C17	440	open	S35
C18	440	closed	Do.
C19	1000	open	Do.
C20	1000	closed	Do.
C21	2000	open	Do.
C22	2000	closed	Do.

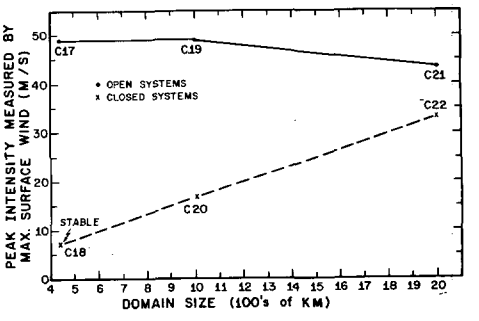

FIGURE 16.—Comparisons of the ultimate intensity attained by model cyclones with open lateral boundaries (C17, C19, and C21) and model cyclones with closed lateral boundaries (C18, C20, and C22) as a function of the radial extent of the computational domain. See table 11 for details.

The 440-km computational domain, used extensively in our experiments (Rosenthal 1969, 1970*a*, 1970*b*), was selected at a very early stage in the design of the model (Rosenthal 1969), based on a need for computational economy. With the selection of this rather limited domain, it was realized that lateral boundary conditions would be extremely important. It was clear that the model hurricane could not be treated as a mechanically closed system since this would force the outflow air to sink relatively close to the storm center and the attendant adiabatic warming would inhibit the development of a warm core system. Empirically, it is well known (Riehl 1954) that upper tropospheric flow patterns that inhibit the escape of outflow air from the near vicinity of tropical disturbances generally are unfavorable for further storm development. The lateral boundary conditions of zeros for the vertical component of relative vorticity, horizontal divergence, and radial gradient of potential temperature were introduced at the very beginning of our experimental program (Rosenthal 1969). The lateral boundary condition of zero radial gradient of specific humidity was added at a later date (Rosenthal 1970*b*) when the explicit water vapor cycle was added. One would hope that it would be possible to reduce the impact of the exact form of the lateral boundary conditions by making the computational domain larger. The material presented below indicates that, if such a domain size exists, it is well in excess of 2000 km. To establish this, comparisons were made between experiments with the original boundary conditions and experiments in which the lateral boundary conditions were approximately those of a smooth, insulated wall. The mathematical expressions are identical to the original ones with the exception that the zero for horizontal convergence is replaced by a zero for the radial wind.

A first experiment with the new (closed) boundary conditions (exp. CC1), otherwise identical to the control, was carried to 504 hr and showed continuous decay from the initial state. In a second experiment (C10), the computational domain was increased to 1000 km but the intensity and scale of the initial perturbation were the same as for the control. With the exception of the lateral boundary conditions, this experiment is identical to C16 (fig. 15, table 9). The results showed a peak intensity of 21 m/s at 384 hr followed by rapid decay.

Since extensions of the computational domain beyond 1000 km with a 10-km radial resolution would have required substantial modifications of the computer program, a new series of experiments (table 11) with 20-km radial resolution was carried out.[4] Figure 16 summarizes the results of these experiments.

Experiment C18 (closed, 440-km domain), identical to CC1 except for radial resolution, also showed monotonic decay (for 504 hr) from the initial conditions. With open boundary conditions, an increase in domain size from 440 to 1000 km produced virtually no change in peak intensity. This is similar to the result obtained above with 10 km resolution. However, a further increase in domain size from 1000 to 2000 km produced a reduction in peak wind of 6 m/s.

The experiments with closed boundaries showed a marked linear increase of peak winds with domain size (if we are allowed to include exp. C18 where peak wind occurs at the initial instant) of about 16 m/s per 1000 km. Linear extrapolation of the two curves on figure 16 (there is, of course, no guarantee that this is valid) shows a crossing point at a domain size of 2500 km. If the curve for closed systems is extrapolated to a peak wind of 50 m/s (that given by the open boundary exp. S35, C17, and C19), this occurs with a domain of about 3000 km.

With 1000-km domains, the open system (C19) reaches its greatest intensity at hour 264 whereas the closed system (C20) does not attain maximum intensity until hour 408. With the 2000-km domain, peak surface winds occur at hour 264 for both sets of boundary conditions (exp. C21 and C22).

Aside from those described above, several other experiments with the closed boundary conditions were run. The

[4] It is not our purpose here to study errors due to radial resolution (see Rosenthal 1970*a*, 1970*b*) and we will not compare the members of the 20-km series with the analogous 10-km experiments.

results of these may be summarized as follows. With a computational domain of 1000 km, peak intensity is strongly dependent on the scale of the initial perturbation (this conflicts with the results obtained with open boundaries). As the scale of the initial perturbation decreases, peak intensity increases until the scale becomes sufficiently small for lateral mixing to dominate. Thereafter, further reduction in scale results in decreases of peak intensity. When the domain size is increased to 2000 km, however, the ultimate intensity is relatively insensitive to the scale of the initial perturbation provided that the latter is not sufficiently small to allow the lateral mixing terms to become dominant.

In agreement with the results obtained with open boundaries, the ultimate intensity of model storms with closed boundaries is relatively insensitive to the strength of the initial perturbation.

7. SUMMARY AND CONCLUSIONS

The experiments can be placed in two broad categories. Those discussed in sections 4 and 5 are mainly concerned with responses to variations in *physical* parameters and attempt to gain deeper insight into the dynamics of tropical cyclones. The experiments discussed in section 6 are mainly concerned with *computational* aspects. These are intended to reveal the biases introduced by some of the arbitrary decisions which were necessary in the design of the model.

The physical parameters examined were those that control the air-sea exchanges of momentum, sensible heat, and latent heat. Many of these experiments yield results in qualitative agreement with experiments performed by Ooyama (1969). In view of the differences between the physical and numerical details of the two models, this is an important result that lends credence to both models.

Perhaps the most striking aspect of the experimental results is the overwhelming dominance, in the immature stage, of the drag coefficient in comparison to the analogous exchange coefficients for sensible and latent heat. This was most vividly portrayed by figure 11. Here, the only significant departures from the control, during the first 48 hr of integration, are in the calculations where the drag coefficient was altered (exp. Q10 and Q18).

The air-sea exchange of latent heat was shown to be a crucial ingredient for development and maintenance of the model storm. It was also found to be far more important than the analogous exchange of sensible heat. A simple extension of Ooyama's (1969) discussion of boundary layer processes (see section 5) provides a plausible explanation for this result.

Experiments in the immature stage showed that linear theory can be somewhat misleading. While, as predicted by linear analysis, the rate of growth during the early periods increased with increasing drag coefficient, the ultimate intensity reached by the model storm varied inversely with the drag coefficient (figs. 8 and 9). In the mature stage, small decreases of drag coefficient lead to stronger peak winds but when the drag coefficient was reduced to zero the peak winds diminished (fig. 10). In the latter situation, it appears that there is insufficient low-level convergence of water vapor to sustain the required convection in the storm core.

The computational experiments revealed a number of interesting points that will be useful in the design of future experiments with tropical cyclone models. With open lateral boundaries and the standard 440-km computational domain, the intensity and structure of model cyclones, when they reached the mature stage, were relatively insensitive to the scale and intensity of the initial vortex (provided that the scale was not so small as to allow lateral mixing terms to become dominant). The time required to reach the mature stage was, however, highly sensitive to initial conditions.

When the size of the computational domain was increased to 1000 km (open lateral boundary) while retaining the initial vortex used for the control, the structure and intensity of the mature model cyclone was again virtually the same as for the control. A further increase in domain size to 2000 km resulted in a 6 m/s reduction of the mature stage peak winds. The structure of the mature cyclone was, however, quite similar to that of the control.

As was to be expected, the lateral boundary conditions proved to be extremely important in determining the life cycle of the model storm. When the zero for horizontal divergence was replaced by a zero for the radial wind, thus converting the open system to one that was mechanically closed, an experiment, otherwise identical to the control, showed monotonic decay from the initial conditions. By increasing the size of the computational domain, it was possible to generate developing model cyclones (closed boundaries). These systems (fig. 16) showed a strong relationship between peak intensity and domain size.

The results summarized by figure 16 suggest that differences due to boundary conditions might be minimized if the domain size were enlarged to something between 2000 and 3000 km. This, however, cannot be guaranteed since no experiments were run with domains larger than 2000 km.

ACKNOWLEDGMENTS

Mr. Robert Carrodus was responsible for drafting and reproducing the figures. Mrs. Mary Jane Clarke typed the manuscript. Computations were performed on the NOAA Control Data Corporation (CDC) 6600 at Suitland, Md., with access made possible through a CDC User 200 remote terminal at the National Hurricane Research Laboratory. Mr. Billy M. Lewis was responsible for the liaison work between Miami and Suitland.

REFERENCES

Anthes, Richard Allen, Rosenthal, Stanley L., and Trout, James W., "Preliminary Results From an Asymmetric Model of the Tropical Cyclone, "*Monthly Weather Review*, Vol. 99, No. 10, Oct. 1971*a*, pp. 744–758.

Anthes, Richard Allen, Trout, James W., and Rosenthal, Stanley L., "Comparisons of Tropical Cyclone Simulations With and Without the Assumption of Circular Symmetry, "*Monthly Weather Review*, Vol. 99, No. 10, Oct. 1971*b*, pp. 759–766.

Byers, Horace Robert, *General Meteorology*, McGraw-Hill Book Co., Inc., New York, N.Y., 1944, 645 pp.

Colón, José A., and Staff, "On the Structure of Hurricane Daisy (1958)," *National Hurricane Research Project Report* No. 48, U.S. Department of Commerce, Weather Bureau, Miami, Fla., Oct. 1961, 102 pp.

Dergarabedian, Paul, and Fendell, Francis, "On Estimation of Maximum Wind Speeds in Tornadoes and Hurricanes," *The Journal of the Astronautical Sciences*, Vol. 17, No. 1, Jan.–Feb. **1970**, pp. 218–236.

Hawkins, Harry F., and Rubsam, Daryl T., "Hurricane Hilda, 1964: II. Structure and Budgets of the Hurricane on October 1, 1964," *Monthly Weather Review*, Vol. 96, No. 9, Sept. **1968**, pp. 617–636.

Hebert, Paul J., and Jordan, Charles L., "Mean Soundings for the Gulf of Mexico Area," *National Hurricane Research Project Report* No. 30, U.S. Department of Commerce, Weather Bureau, Miami, Fla., Apr. **1959**, 10 pp.

Kuo, H.-L., "On Formation and Intensification of Tropical Cyclones Through Latent Heat Release by Cumulus Convection," *Journal of the Atmospheric Sciences*, Vol. 22, No. 1, Jan. **1965**, pp. 40–63.

Malkus, Joanne S., and Riehl, Herbert, "On the Dynamics and Energy Transformations in Steady-State Hurricanes," *Tellus*, Vol. 12, No. 1, Stockholm, Sweden, Feb. **1960**, pp. 1–20.

Matsuno, Taroh, "Numerical Integregations of the Primitive Equations by a Simulated Backward Difference Method," *Journal of the Meteorological Society of Japan*, Ser. 2, Vol. 44, No. 1, Tokyo, Feb. **1966**, pp. 76–84.

Miller, Banner I., "On the Momentum and Energy Balance of Hurricane Helene (1958), "*National Hurricane Research Project Report* No. 53, U.S. Department of Commerce, Weather Bureau, Miami, Fla., Apr. **1962**, 19 pp.

Ooyama, Katsuyuki, "Numerical Simulation of the Life-Cycle of Tropical Cyclones," *Journal of the Atmospheric Sciences*, Vol. 26, No. 1, Jan. **1969**, pp. 3–40.

Palmén, Erik Herbert, "On the Formation and Structure of Tropical Hurricanes," *Geophysica*, Vol. 3, No. 26, Helsinki, Finland, **1948**, pp. 26–38.

Ramage, Colin S., "Comments on 'Numerical Simulation of the Life-Cycle of Tropical Cyclones,'" *Journal of the Atmospheric Sciences*, Vol. 27, No. 3, May **1970** pp. 506–507.

Riehl, Herbert, *Tropical Meteorology*, McGraw-Hill Book Co., Inc., New York, N.Y., **1954**, 392 pp.

Riehl, Herbert, and Malkus, Joanne S., "Some Aspects of Hurricane Daisy, 1958," *Tellus*, Vol. 13, No. 2, Stockholm, Sweden, May **1961**, pp. 181–213.

Rodenhuis, David, "A Note Concerning the Effect of Gravitational Stability on the CISK Model of Tropical Disturbances," *Journal of the Atmospheric Sciences*, Vol. 28, No. 1, Jan. **1971**, pp. 126–129.

Roll, Hans Ulrich, *Physics of the Marine Atmosphere*, Academic Press, New York, N.Y., **1965**, 426 pp.

Rosenthal, Stanley L., "Numerical Experiments With a Multilevel Primitive Equation Model Designed to Simulate the Development of Tropical Cyclones: Experiment I," *ESSA Technical Memorandum* ERLTM–NHRL 82, U.S. Department of Commerce, National Hurricane Research Laboratory, Miami, Fla., Jan. **1969**, 36 pp.

Rosenthal, Stanley L., "Experiments With a Numerical Model of Tropical Cyclone Development—Some Effects of Radial Resolution," *Monthly Weather Review*, Vol. 98, No. 2, Feb. **1970***a*, pp. 106–120.

Rosenthal, Stanley L., "A Circularly Symmetric Primitive Equation Model of Tropical Cyclone Development Containing an Explicit Water Vapor Cycle," *Monthly Weather Review*, Vol. 98, No. 9, Sept. **1970***b*, pp. 643–663.

Rosenthal, Stanley L., and Koss, Walter J., "Linear Analysis of a Tropical Cyclone Model With Increased Vertical Resolution," *Monthly Weather Review*, Vol. 96, No. 12, Dec. **1968**, pp. 858–866.

Sundqvist, Hilding, "Numerical Simulation of the Development of Tropical Cyclones With a Ten-Level Model, Part I." *Tellus*, Vol. 22, No. 4, Stockholm, Sweden, July **1970**, pp. 359–390.

Yamasaki, Masanori, "Detailed Analysis of a Tropical Cyclone Simulated With a 13-Layer Model," *Papers in Meteorology and Geophysics*, Vol. 19, No. 4, Tokyo, Japan, Dec. **1968**, pp. 559–585.

[*Received December 2, 1970; revised March 9, 1971*]